

Fabrication of arrayed glassy carbon field emitters

Yasunari Sohda,^{a)} David M. Tanenbaum, Stephen W. Turner, and Harold G. Craighead
School of Engineering and Applied Physics, Cornell University, Ithaca, New York 14853

(Received 9 September 1996; accepted 17 January 1997)

Glassy carbon has desirable properties for electron field emission such as surface inertness, electrical conductivity, and thermal stability. In addition, a uniform thick substrate with a polished surface is easily obtainable. This enables one to apply large scale integrated circuit processing for fabricating arrayed tips. By using oxygen reactive ion etching, cusps over 3.5 μm in height and 2.5 μm in base diameter are fabricated with a tip radius of under 10 nm. The process is assisted by the formation of a layer of etch products which protects the newly forming tip from bending and over etching. The field emission current up to 50 μA from the glassy carbon tips is obtained by applying high voltage to a mesh anode. The current which passed through the mesh anode is collected at another electrode and measured. The Fowler–Nordheim plot suggests the existence of nm scale structure on the tip. This favorable result indicates glassy carbon substrate is a good substrate for field emitter arrays. © 1997 American Vacuum Society. [S0734-211X(97)06402-0]

I. INTRODUCTION

After the stimulation of the work of Spint,¹ there has been a great deal of research in the area of arrayed field emitters. The most popular substrate has been silicon² because the fabrication processes have been well developed for silicon large scale integrated circuit (LSI). Silicon has advantages such as large single crystal structure and a variety of etching methods. Thus, tips have been made from silicon, and films deposited on silicon substrates or over silicon tip structures.^{3–5} However, it is not yet clear if silicon can realize good emission properties because its surface is relatively active. In addition, for deposited films, one must assure the uniformity of the film, which is even more difficult in the case of polycrystalline materials.

In this article, the authors propose glassy carbon as a new substrate for vacuum microelectronics. Carbon has been investigated as an emitter material because of its surface inertness and high thermal stability.^{6–8} Currently diamond and diamondlike films are intensively investigated because of their apparent negative electron affinity.^{9,10} Compared to diamond film, glassy carbon has some advantages.¹¹ Glassy carbon can be characterized as an exclusively sp^2 binding, graphitelike material. It has good electrical conductivity, while diamond is normally an insulator. In addition, uniform polished substrates can be easily obtained, whereas it is still a major problem to deposit thick and uniform diamond film. Because of these features, LSI processes can be applied to fabricate emitters. This substrate is inexpensive and commercially produced. These qualities are important for practical application.

The work function of glassy carbon is considered to be similar to graphite, that is, about 4.6 eV.¹² Though this large work function may reduce modification by surface adsorption of atmospheric molecules, it necessitates high electric fields to obtain field emission. Thus, the possibility of fabri-

cating small tip radius is one of the most important issues in glassy carbon field emitters. Glassy carbon has been also investigated as an electron emitter.^{13,14} However, in this research, there was a single emitter and the tip radius was large. In this article, the feasibility of fabricating arrayed small emitter tips by using glassy carbon substrates and LSI processes is demonstrated. In addition, preliminary field emission data is shown.

II. EXPERIMENTAL PROCEDURE

The glassy carbon substrate used was a 50 mm \times 50 mm \times 1 mm thick plate. This is commercially available from Johnson Matthey (Alfa[®]: Glassy carbon plate type 1), which is produced by thermal decomposition of crosslinked synthetic resin at 1100°. Because it has good electrical conductivity ($< 10^{-3} \Omega \text{ cm}$) and heat durability in vacuum, it is a suitable material for field emitters. The uniformity of the thickness was within $\pm 10 \mu\text{m}$ and the surface roughness was within $\pm 0.02 \mu\text{m}$. These parameters are within the acceptable range for LSI processing. Figure 1 shows the process flow. First, 0.25- μm -thick SiO_2 film was deposited by plasma enhanced chemical vapor deposition (CVD) (PECVD) on the glassy carbon as an etch mask. Next, a square array of 2.5- μm -diam circles was delineated in 0.5- μm -thick resist by photolithography. The array spacing was 10 μm . Then, SiO_2 was etched by reactive ion etching (RIE) with 96% CHF_3 /4% O_2 gas. The rf power density and gas pressure were 0.34 W/cm^2 and 40 mTorr, respectively. The glassy carbon was etched by the same RIE etcher with oxygen etchant. The rf power and gas pressure are 0.25 W/cm^2 and 0.3–0.6 Torr, respectively. The reason for using RIE is that the ratio of vertical and horizontal etch rates can be controlled by etch pressure. Residual resist was removed during the etch process. After that, the SiO_2 mask was removed by a 6:1 buffered high frequency (hf) (BHF) etch.

The surface of the glassy carbon was analyzed by scanning Auger electron spectroscopy. The electron energy was 10 kV and the electron current was 10 nA.

^{a)}On leave from Hitachi Ltd., Japan; Electronic mail: sohda@crl.hitachi.co.jp

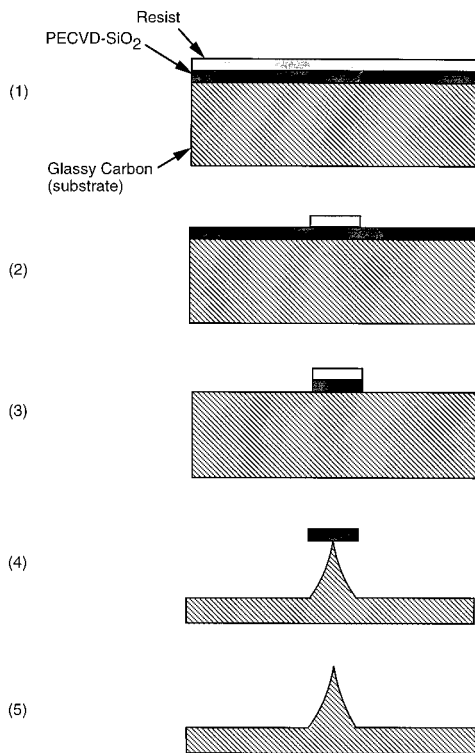


FIG. 1. The fabrication flow of glassy carbon cusps where the LSI process is applied. (1) Deposition and spin coating; (2) photolithography; (3) RIE(CHF_3, O_2); (4) RIE(O_2); (5) buffered HF etching.

Field emission was evaluated in an ultrahigh vacuum chamber, the base pressure was 3×10^{-10} Torr. The sample was cured in 10^{-6} Torr vacuum at 900 degrees before insertion to the chamber. High voltage was applied to a mesh anode with 60% open space. The gap between the sample and the anode was $160 \pm 10 \mu\text{m}$. Field emission was detected by measuring the current which cleared the mesh and was collected by the third electrode. The third electrode was 20 mm apart from the mesh and had the same voltage of the mesh.

III. RESULTS AND DISCUSSION

A. Fabricated arrayed tips

Figures 2(a) and 2(b) show the scanning electron microscopy (SEM) photographs of the fabricated arrayed carbon cusps, bird's eye view of the single cusp, side view of the single cusp, and enlarged tip, respectively. Each cusp is different from every other. The oxygen etching gas pressure of 0.6 Torr is 10 times larger than ordinary gas pressure for anisotropic etching of 0.06 Torr. This high pressure enables partially anisotropic undercutting, which is responsible for the cusp shape. The glassy carbon was easily etched by oxygen plasma. The vertical etching rate was 40 nm/min. It can be seen that arrayed cusps are uniformly fabricated. The cusp height is $3.5 \mu\text{m}$ and the diameter of the cusp is $2.5 \mu\text{m}$. In addition, the etching ratio between SiO_2 and glassy carbon was over 100. Thus, the mask shape was essentially the same

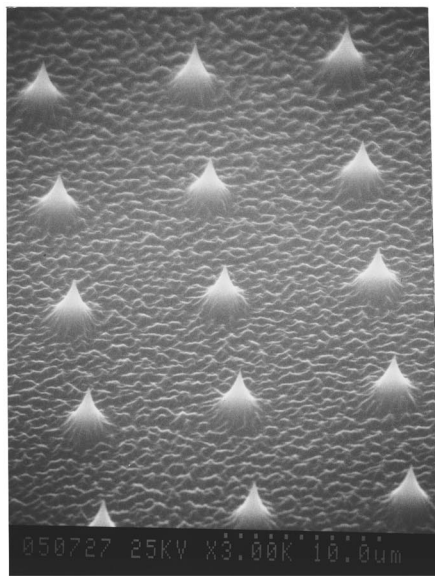
during etching. As a result, an etch ratio between horizontal and vertical of 3:1 was obtained. That is partial anisotropic etching. This ratio can be changed by changing gas pressure. For example, an etch ratio of about 6:1 was obtained at 0.3 Torr. It can be also seen that the etched plane has about $0.2 \mu\text{m}$ roughness. This is considered to be due to redeposition of sputtered mask or electrode materials on the sample that is often seen in high selectivity RIE. However, the surface of cusp is not so rough because the SiO_2 is also a mask for redeposition. In addition, the tip radius is typically under 10 nm. This is comparable to that of conventional silicon tips. In addition, this small radius is also seen even if they were overetched.

Figure 3 shows the SEM side view of a glassy carbon cusp etched by adding 1.25% CHF_3 to etch the redeposited materials. The etch depth is also $3.5 \mu\text{m}$. The etched plane surface roughness is improved from $0.1 \mu\text{m}$ order to $0.01 \mu\text{m}$ order. In this case, the tip surface is also smoother. On the other hand, selectivity reduced to about 10. Thus, the SiO_2 mask was being damaged during etching. As a result, the cusp was overetched and the height in Fig. 3 is $2.5 \mu\text{m}$. To fabricate a tall cusp as in Fig. 2, the etch parameters, as well as the mask design must be carefully optimized.¹⁵ Another technique is to begin by etching the carbon with oxygen only and finish with oxygen and CHF_3 . In both methods, it should be noted that a decrease in the etch selectivity can deteriorate process reproducibility.

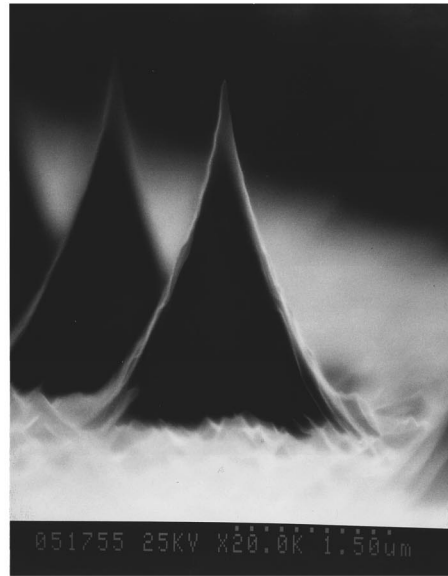
Figure 4 shows an SEM micrograph of an over etched sample in the same etching condition of Fig. 2, but before BHF etching. The SiO_2 mask remains on the cusp and there is something between the cusp and the SiO_2 disk, which appears from the SEM contrast to be low density material. This low density material is also observed in the planar areas, however, it is not seen after BHF etching. This intermediate product is very important to the fabrication of sharp tips. This suspends the SiO_2 mask even during over etching. Thus, this avoids bending of the cusp under the weight of the SiO_2 disk before etch completion and also protects the tip from vertical etching during over etch. As a result, sharpness of the tip is realized over a wide range of etch depth. This is also expected to make process control easy. The effect is like oxidation sharpening in silicon tip fabrication.²

B. Auger spectra's analysis

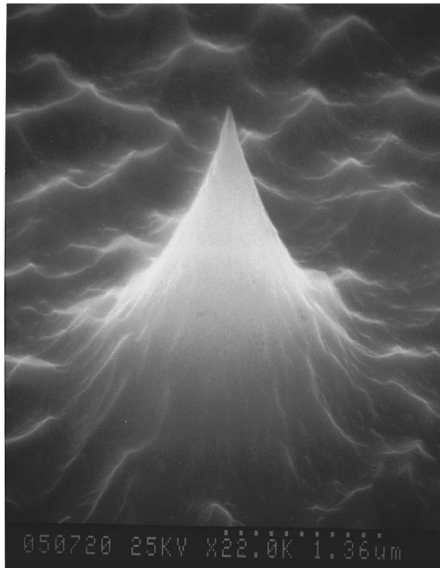
In order to investigate the intermediate material mentioned above, scanning Auger electron analysis has been applied. Figures 5(a)–5(c) show the spectra of the tip surface before BHF etching, the nonetched glassy carbon surface and the tip surface after BHF etching. It can be seen that the tip surface before BHF etching consists of mainly carbon and oxygen. In addition, there is more oxygen compared to the nonetched surface. According to calculations of atomic concentration from the spectra, the oxygen concentrations of (a), (b), and (c) are 15.4%, 3.9%, and 4.8%, respectively. Although the carbon surface is relatively inert, there are still many active sites such as dangling bonds.¹⁶ It is well known that oxygen adsorbs at these sites.¹⁷ Thus, it is not surprising



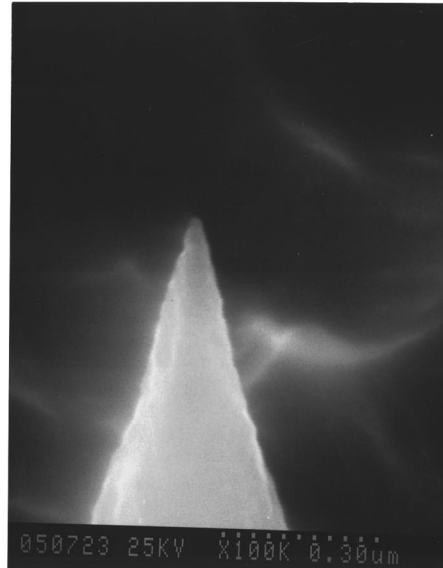
(a)



(c)



(b)



(d)

FIG. 2. SEM photographs of arrayed glassy carbon cusps. Glassy carbon arrayed cusps with tip radius of under 10 nm have been fabricated by oxygen reactive ion etching. The array spacing is 10 μm . The height and the base diameter of each cusp is 3.5 and 2.5 μm , respectively. (a) Arrayed cusps, (b) a single cusp (bird's eye view), (c) a single cusp (side view), and (d) an enlarged tip photograph.

to observe oxygen in the nonetched surface. However, the large percent of oxygen in (a) suggests the low density material between the tip and the mask is an intermediate reaction product of the oxygen etchant and the glassy carbon substrate. However, it is still not volatile. In addition, because the spectra of (b) and (c) are almost the same, this low density material is completely removed by the subsequent BHF etching. As a result, the oxygen concentration at the tip surface after BHF etching is the similar to that of the non-etched surface. From these results, it is indicated that glassy carbon etching makes an intermediate product on the surface.

However, the boundary between nonetched surface and the intermediate product is very clear. Thus, this does not interfere with fabrication of a sharp tip. The carbon spectra of the nonetched surface and the tip array after BHF etching are similar to graphite.¹⁸ This is reasonable because glassy carbon is similar in structure to graphite.

Figure 6 is an enlargement of the Auger spectra of the tip surface, before BHF etching (a), nonetched surface (b), and after BHF etching (c) in the region of the carbon 1s peak. The spectra are not differentiated. The spectra of the non-etched surface and the tip array after BHF etching are almost

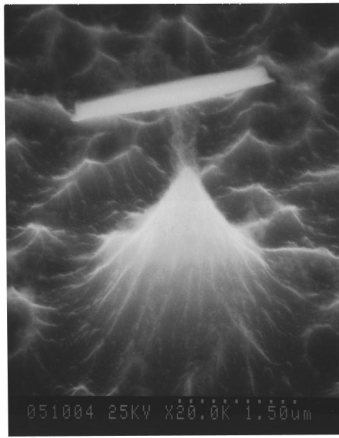


FIG. 3. A SEM side view of a single cusp etched by adding CHF_3 . The surface roughness is improved.

the same. The interesting thing is that many additional peaks are clearly observed with a large energy shift on the tip surface before BHF etching. In particular, there is a large peak at 20 eV above the graphite peak. This peak has no tail to its lower energy side. These suggest that there are structures on the surface which have low binding energy electrons.¹⁹ This could be due to the presence of much oxygen on the surface, however, it is not yet clear to us what kind of binding structure of carbon and oxygen realizes these peaks. Further analysis is expected to clarify the etch mechanism.

C. Field emission experiment

In the field emission experiment, the sample that was etched in 0.3 Torr oxygen gas was used. The purpose is to fabricate a taller cusp for greater enhancement of the electric field. The height of the approximately 14 000 cusps in this sample is 5 μm . At first, the current voltage curve was not stable. However, after several times of voltage cycle, the stability was improved. Figure 7(a) shows the current–voltage plot of the measured current where the current was detected starting around 1000 V. Figure 7(b) is the Fowler–Nordheim plot of the current. The almost linear curve indi-

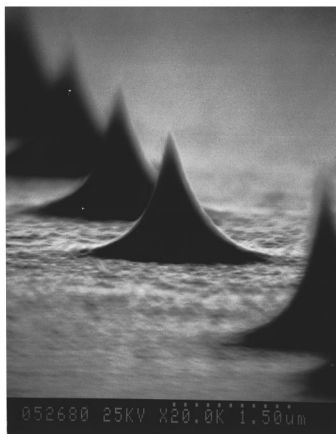


FIG. 4. A SEM bird's eye view of an over etched sample. There is low density material between the cusp and the SiO_2 mask.

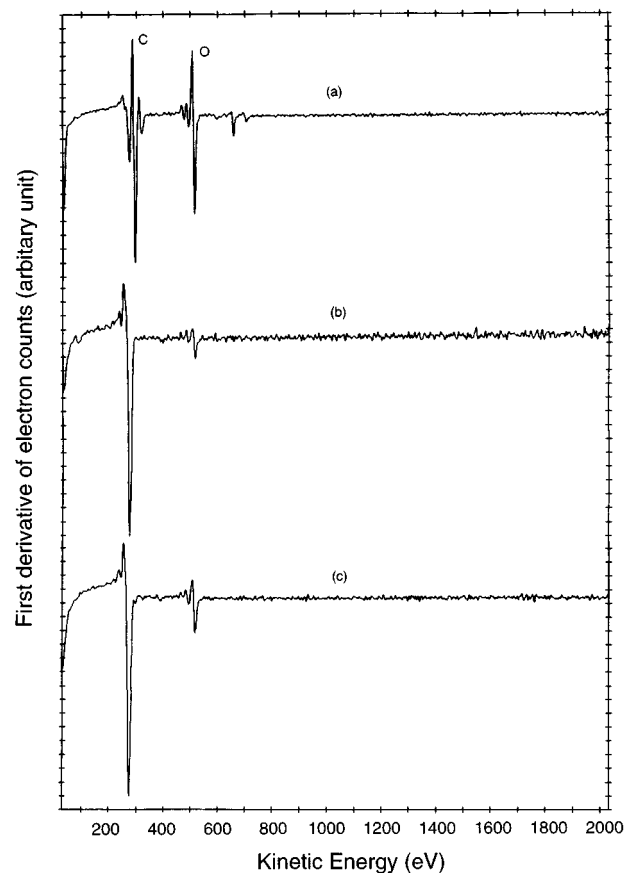


FIG. 5. Differentiated Auger spectra of various surfaces. There is much oxygen on the glassy carbon surface after O_2 etching. However, this is removed by BHF etching. (a) Carbon tip before BHF etching, (b) nonetched carbon, and (c) carbon tip after BHF etching.

cates the current is due to field emission. However, there may be a slightly different slope at the highest voltage. This could be due to the contribution of tips with larger tip radius. The Fowler–Nordheim plot is analyzed by the following equation:²⁰

$$J = \frac{1.4 \times 10^{-6} \beta^2 V^2}{\phi} \exp\left(-6.53 \times 10^7 \frac{\phi^{3/2}}{\beta V}\right) \times \exp\left(\frac{9.87}{\phi^{1/2}}\right), \quad (1)$$

where J is the current density (A/cm^2), V is the anode voltage (V), f is the work function (eV), and b is the electric field enhancement factor.

Assuming that the work function is the same as 4.6 eV of graphite, b is $4.1 \times 10^4 (1/\text{cm})$. This large value of b , implies a very small tip radius. The electric field at the tip was simulated by commercially available software.²¹ Assuming the cusp is a cone of 5 μm height and 2.5 μm diameter, a tip radius of 2 nm is necessary to obtain the measured b . The electron current from this tip is calculated as 30 nA at 1300 V. Because open space of the mesh anode is 60%, the actual emission current is considered to be 42 μA at 1300 V. This indicates there are 1.4×10^3 emission centers in the experi-

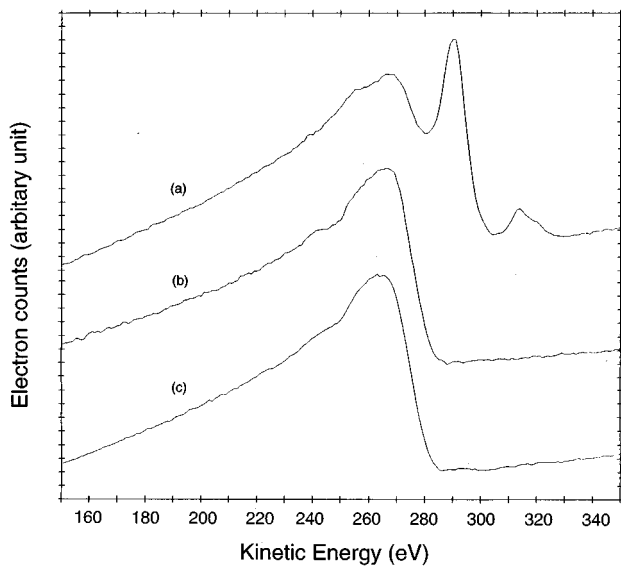


FIG. 6. Nondifferentiated Auger spectra in the region of the carbon 1s peak. There are many additional peaks before BHF etching. (a) Carbon tip before BHF etching, (b) nonetched carbon, and (c) carbon tip after BHF etching.

ment. In addition, the emission area is calculated as $5.6 \times 10^{-11} \text{ cm}^2$ from the Fowler–Nordheim plot. If this area is divided by the area of a circle with a 2 nm radius, a similarly large number of 7.4×10^2 is obtained (corrected by

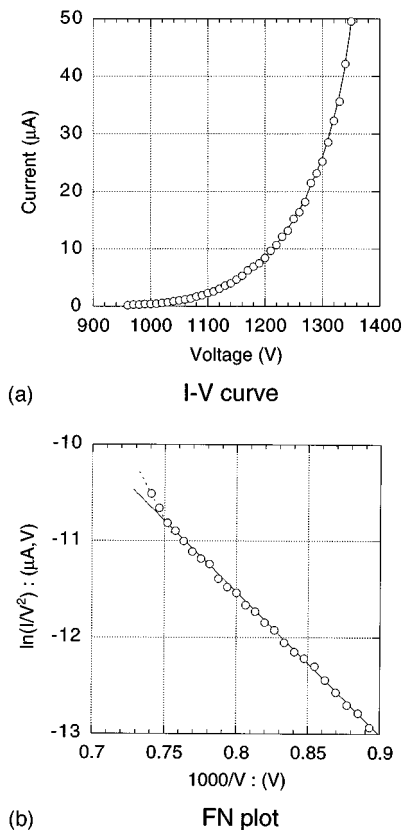


FIG. 7. Field emission current from glassy carbon tip array. (a) Voltage–current plot and (b) Fowler–Nordheim plot.

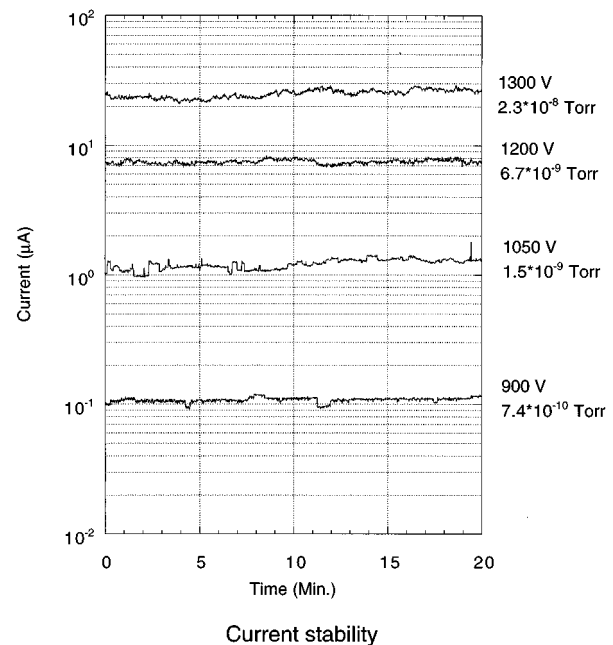


FIG. 8. Current stability at various currents. As the current increases, the noise type changes from flip-flop type to flicker type.

60% transmittance). Although the work function of the tip is not clear, its effect on the estimated tip radius and number of the emitting points is roughly $\phi^{-3/2}$ and $\phi \exp(-9.87/\phi^{1/2})$, respectively. Thus, small errors in the work function will not change the order of magnitude of the radius or number of emitting points. However, it is difficult to know how many cusps emit in this experiment, because there can be many small emitting points on one cusp. Field emission from small tip structures was reported in other materials²² and there is also a related simulation report.²³ The observation of a single fabricated cusp is planned to address these issues.

Figure 8 shows the emission current stability at various currents. In the lower current region, flip-floplike noise is observed. This noise is often seen in carbon emitters.^{14,24} However, in the higher current region, the ratio of noise decreases and becomes flicker type. The noise is $\pm 10\%$ at $7 \mu\text{A}$. Two possible reasons for this difference are considered. First, the number of emitting point is likely to be increased. This may average the noise of each point. Second, the chamber pressure worsens because of electron bombardment. This may increase the population of high mobility adsorbates on the tip and increase flicker type noise. However, the initial surface condition is not clear, because the sample surface is not cleaned in the experiment chamber. The maximum temperature in the chamber is only 150° at baking for ultrahigh vacuum. Because oxygen and carbon–oxide on the glassy carbon surface is not removed at this temperature,¹⁴ the initial surface condition of the tip is not ideal. An improvement of the experimental equipment is necessary. The emission was constantly observed during a day. However, the experiment of the long-time reliability is also a remaining issue.

IV. CONCLUSIONS

Glassy carbon arrayed cusps with tip radius of under 10 nm have been fabricated by oxygen reactive ion etching. The height is over 3.5 μm and the diameter is 2.5 μm . An intermediate product of the reactive ion etch appears to assist the fabrication by mechanically stabilizing the narrow tip of the cusp, and holding the SiO_2 etch mask in place even during over etch. In addition, it can be removed by buffered HF etching.

The field emission current up to 50 μA from the glassy carbon tips through the mesh electrode was also obtained. According to the Fowler–Nordheim plot, the existence of nm size tips was suggested. The number of the emission point was estimated as about 10^3 . The stability was $\pm 10\%$ at 7 μA . As a result, glassy carbon is considered to be a promising candidate for practical arrayed field emitters. Further experiment is necessary to investigate the etching mechanism and field emission properties.

ACKNOWLEDGMENTS

The authors would like to acknowledge the Cornell Nanofabrication Facility (CNF) for fabricating an arrayed glassy carbon cusp. Y. Sohda would like to acknowledge helpful discussion of fabrication process and Auger spectrum analysis with Dr. P. M. St. John of Cornell University.

¹C. A. Spindt, I. Brodie, L. Humphrey, and E. R. Westerberg, *J. Appl. Phys.* **47**, 5248 (1976).

²For example, S. Kanemura, T. Hirano, H. Tanoue, and J. Itoh, *J. Vac. Sci. Technol. B* **14**, 1885 (1996).

³C. G. Lee, H. Y. Ahn, B. G. Park, and J. D. Lee, *J. Vac. Sci. Technol. B* **14**, 1966 (1996).

⁴J. P. Spallas, R. D. Boyd, J. A. Britten, A. Fernandez, A. M. Hawryluk, M. D. Perry, and D. R. Kania, *J. Vac. Sci. Technol. B* **14**, 2005 (1996).

⁵P. R. Schwoebel, C. A. Spindt, and I. Brodie, *J. Vac. Sci. Technol. B* **13**, 338 (1995).

⁶A. F. Myers, S. M. Camphausen, J. J. Cuomo, J. J. Hren, J. Liu, and J. Bruley, *J. Vac. Sci. Technol. B* **14**, 2024 (1996).

⁷S. Bajic and R. V. Latham, *J. Phys. D* **21**, 200 (1988).

⁸M. A. More and D. S. Joag, *J. Phys. D* **25**, 1844 (1992).

⁹E. I. Givargizov, V. V. Zhirnov, A. V. Kuznetsov, and P. S. Plekhanov, *J. Vac. Sci. Technol. B* **14**, 2030 (1996).

¹⁰F. J. Himpsel, J. A. Knapp, J. A. Van Vechten, and D. E. Eastman, *Phys. Rev. B* **20**, 624 (1979).

¹¹W. E. Van der Linden and J. W. Dieker, *Anal. Chim. Acta* **199**, 1 (1980).

¹²H. F. Ivey, *Phys. Rev.* **76**, 567 (1949).

¹³S. Hosoki, S. Yamamoto, M. Futamoto, and S. Fuhuhara, *Surf. Sci.* **86**, 723 (1979).

¹⁴S. Yamamoto, S. Hosoki, M. Futamoto, and S. Fuhuhara, *Surf. Sci.* **86**, 734 (1979).

¹⁵M. R. Rakhshanderoo and S. W. Pang, *J. Vac. Sci. Technol. B* **14**, 612 (1996).

¹⁶J. B. Donnet, *Carbon* **6**, 161 (1968).

¹⁷M. Futamoto, S. Hosoki, and U. Kawabe, *Surf. Sci.* **86**, 718 (1979).

¹⁸T. W. Haas, J. T. Grant, and G. J. Dooley III, *J. Appl. Phys.* **43**, 1853 (1972).

¹⁹D. E. Ramaker, N. H. Turner, and J. Milliken, *J. Phys. Chem.* **96**, 7627 (1992).

²⁰D. Hong, M. Aslam, M. Feldmann, and M. Olinger, *J. Vac. Sci. Technol. B* **12**, 764 (1994).

²¹X. Zhu and E. Munro, *J. Vac. Sci. Technol. B* **7**, 1862 (1989).

²²E. C. Boswell, M. Huang, G. D. W. Smith, and P. R. Wilshaw, *J. Vac. Sci. Technol. B* **14**, 1895 (1996).

²³H. W. P. Koops, M. Weber, J. Urban, and C. Schossler, *Proc. SPIE* **2522**, 189 (1995).

²⁴M. A. More and D. S. Joag, *J. Phys. D* **25**, 1844 (1992).